Can Managed Aquifer Recharge Mitigate the Groundwater Overdraft in Central Valley, California?

Sarfaraz Alam[1*], Mekonnen Gebremichael[1], Ruopu Li[2], Jeff Dozier[3], and Dennis P Lettenmaier[4]

[1]Department of Civil and Environmental Engineering, University of California, Los Angeles, CA, USA. [2]School of Earth Systems and Sustainability, Southern Illinois University-Carbondale, Carbondale, IL, USA. [3]Bren School of Environmental Science & Management, University of California, Santa Barbara, CA, USA. [4]Department of Geography, University of California, Los Angeles, CA, USA

Corresponding author: Sarfaraz Alam (szalam@ucla.edu)

Key Points:

- The impact of managed aquifer recharge (MAR) on Central Valley's (CV) groundwater storage varies among regions.
- In the southern CV where the groundwater depletion problem is large, MAR can recover a small portion of the existing groundwater overdraft.
- Delivery of excess winter flow from northern CV to the south for MAR can mitigate a greater portion of existing groundwater overdraft.

Abstract

Groundwater plays a critical role in sustaining agriculture in California's Central Valley (CV). However, groundwater storage in the CV has been declining by around 3 km^3/year over the last several decades, with much larger declines during the 2007-2009 and 2012-2015 droughts. California's Sustainable Groundwater Management Act (SGMA) mandates that this imbalance be eliminated. Managed Aquifer Recharge (MAR) can potentially mitigate existing overdraft by recharging excess streamflow (during flood periods) to the aquifers. However, it is unknown to

what degree the existing CV groundwater overdraft might be mitigated by MAR. We applied a coupled surface water-groundwater simulation model to quantify the groundwater overdraft recovery that could be accomplished by MAR. We conducted numerical experiments with multiple water allocation scenarios that apply excess streamflow (viz. flow exceeding 90th and 80th percentiles) constrained by the maximum depth of applied water in recharge areas (viz. 0.61m and 3.05m). Our results show that MAR could recover 9%-22% of the existing groundwater overdraft CV-wide based on a 56-year simulation (1960-2015). The impact of MAR varies among regions. In southern CV where groundwater depletion is a major problem, the contribution of MAR to the overdraft recovery would be less, only 2.7%-3.3% in Tulare (TL) and 3.2%-7.8% in San Joaquin (SJ). However, moving excess winter flow from the northern CV to the south for MAR would increase the overdraft recovery to 30% in SJ and 62% in TL. Our results also show that MAR would supplement summer low flows (52%-73%, CV-wide) and reduce flood peaks.

Plain Language Summary

California's Central Valley has experienced chronic groundwater depletion over the past half century. One mitigation strategy that has been widely suggested is to use excess winter (flood) flows for groundwater banking (a.k.a., Managed Aquifer Recharge or MAR). We estimate how much of the existing groundwater overdraft could be mitigated by implementation of MAR. We conducted numerical experiments to assess groundwater storage changes in response to selected MAR scenarios. Overall, MAR could recover most of the historical overdraft in the Sacramento and east of Delta sub-basins, but much less in the San Joaquin and Tulare sub-basins (where groundwater overdrafts are greatest) where there is less excess water available for MAR. Moving excess flood waters from the Delta to the southern sub-basins would result in much greater

aquifer recovery in those areas where historic overdrafts have been the greatest. Moreover, we find that MAR would have important ancillary benefits, including augmentation of low flows and flood risk reduction.

1 Introduction

Groundwater is an important freshwater source for more than 1.5 billion people globally (Alley et al., 2002). As the population grows and irrigated agriculture expands, the reliance on groundwater resources continues to increase (Rodell et al., 2009; Gorelick & Zheng, 2015; Siebert et al., 2010). The overexploitation of groundwater due to increasing demand and climate-related factors (i.e. drought) in recent decades has had major, sometimes irreversible, impacts to many aquifers around the world (Taylor et al. 2013). For example, according to Wada et al. (2010), groundwater storage depletion rates have doubled over the past 50 years in arid and semi-arid regions of the world. Such large-scale depletion threatens sustainable agricultural development, as well as environmental and ecological health. Climate change is likely to increase groundwater depletion rates by increasing crop water use and altering the timing and volume of surface water flows (Alam et al., 2019; Hanson et al., 2012). Therefore, there is a critical need to identify vulnerable locations most affected by groundwater overdraft, and potential measures to mitigate existing groundwater depletion.

The Central Valley of California (CV), our study region, is one of the most agriculturally productive regions in the USA (Figure 1). It produces more than half of the fruits, nuts and vegetables grown in U.S. Almost all agricultural lands in the CV are irrigated, using surface water, groundwater, or a combination of both. Surface water comes from upstream watersheds that surround the CV, the availability of which generally decreases from the north to the south

following a north-south precipitation gradient. The regional imbalance in surface water supply is mitigated somewhat by a complex surface water transfer network (Brown et al., 2009). Nonetheless, surface water alone is insufficient to meet water demands, and the deficit has been met by groundwater exploitation (Li et al., 2018; Famiglietti et al., 2011). Historically, groundwater has played a vital role in sustaining high agricultural productivity in the CV, especially during drought years.

Overexploitation of groundwater in the CV over the past 60 years (1950-2009) has resulted in an average depletion rate of around 3 km^3/year (Alam et al., 2019). The depletion rate more than doubled during the recent prolonged droughts (2007-2009, and 2012-2015) (Xiao et al., 2017). Moreover, climate change by the end of this century is expected put additional pressure on the aquifer, causing an additional depletion rate of 2 ±1.4 km^3/year (Alam et al. 2019). To minimize the impact of climate change and ensure groundwater sustainability, the California legislature passed the Sustainable Groundwater Management Act (SGMA) in 2014 to regulate the use and application of groundwater resources and to restore groundwater level to an "acceptable level" by 2042.

Several mitigation measures have been proposed to replenish the existing groundwater overdraft, including management of demand and supply of water resources (Hanak et al., 2010). A key mitigation measure that has been proposed by California's Department of Water Resources (CDWR) is Managed Aquifer Recharge (MAR), which would uses excess flood flows (termed Flood-MAR) in the wet seasons to replenish groundwater via artificial recharge, primarily in the form of seasonal land flooding (CDWR, 2019; Sprenger et al., 2017). The benefits of MAR have been recognized, leading to widespread interest (Dillon et al., 2019). MAR has the potential to replenish aquifers, reduce land subsidence risk, increase drought resilience and lower flood

related risks (Chinnasamy et al., 2018; Niswonger et al., 2017; Ronayne et al., 2017; Scanlon et al., 2016; Hashemi et al., 2015). MAR studies in California and elsewhere conducted at the local and farm levels (e.g., Ghasemizade et al., 2019; Kourakos et al., 2019; Dahlke et al., 2018; Bachand et al., 2014) demonstrate that such practices are scalable to the river basin level. However, the benefits and limitations of MAR implementation at the scale of the entire CV are not well understood. There remain key questions, such as, the extent to which MAR can replenish existing groundwater overdraft in the CV, and which regions have the greatest potential for MAR.

Here, we address the question of how much of the CV's groundwater overdraft can potentially be mitigated by MAR and how much the recovery is likely to vary among regions and subregions of the CV. In addition, we examine the additional benefits of MAR for low flow augmentation and flood reduction.

2 Study Area

Figure 1a-b shows the location of the CV region of California, which covers an area of around 53,600 km^2. As can be seen in Figure 1c, the CV generally has low relief, and is surrounded by high-elevation watersheds (hereafter headwater watersheds) in the Sierra Nevada, which are the source of most of the surface water flows to the CV. Surface water entering the CV from headwater watersheds flows through natural stream networks, and that part that is not diverted for irrigation eventually enters the San Francisco Bay Delta (hereafter Delta) to the west.

As shown in Figure 1c, the CDWR divides the CV into five major hydrologic regions: Sacramento (SC; 15,900 km^2 watershed area), Delta (DL; 2,900 km^2), East Delta (EZ; 3,660 km^2), San Joaquin (SJ; 10,020 km^2), and Tulare (TL; 21,200 km^2). The Sacramento region is

located in the northern part, Tulare in the southern part, and San Joaquin in the middle. The Delta and East-Delta hydrologic regions are located near the center of the CV, and provide outlets to the Delta that drain excess surface water (water remaining that is not diverted for agricultural or municipal use) flowing through the rivers in the CV. As shown in Figure 1d, CDWR has further divided the region into 21 subregions for hydrologic studies. Here, we refer to each subregion using the IDs shown in Figure 1d, e.g. subregion 1 will be referred to as SR1.

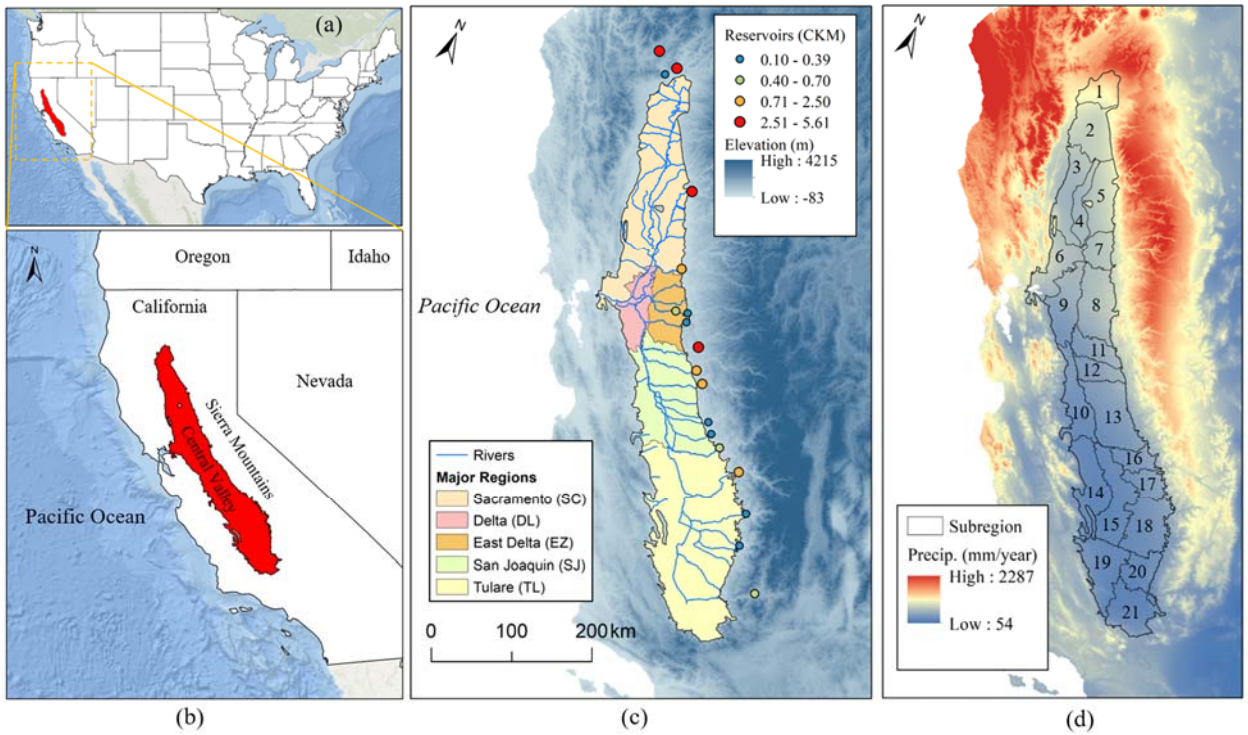

Figure 1. (a) Location of the Central Valley (CV) in the US; (b) CV location in California, (c) major hydrologic regions (HR), major reservoirs and river networks within the CV. Blue shade represents elevation; and (c) 21 subregions (SR) of the CV, where the numbers represent the ID of each subregion. Red to blue shade represents annual average precipitation (mm/year) obtained from WorldClim global climate data (http://worldclim.org/).

The long term rainfall map (Figure 1d) shows that there is a strong precipitation gradient from the headwater watersheds to the valley floors, and from the northern part of the region (which is mostly semi-humid) to the southern part (which is mostly semi-arid). The headwater watersheds in the north are generally rain-dominated and contribute most of the surface water flowing to the CV, while the southern headwater basins are snow-dominated. These contrasts motivated the construction of a complex network of surface storage and conveyance structures (mostly completed by the 1970s) to mediate the north-south imbalance.

There is also a temporal mismatch between rainfall and crop seasons: most of the precipitation falls from November to March, while irrigation demand is mostly in summer (July to September). This mismatch has been mitigated by some 18 major headwater reservoirs (locations shown as circles in Figure 1c), which store winter flows for release during the summer (Alam et al., 2019). In addition to providing water during low-flow season, the reservoirs provide additional benefits in the form of flood protection and environmental services. The surface water that enters the CV is diverted at several locations to satisfy agricultural, municipal and environmental needs taking into account water rights and legal requirements. The excess water, i.e. the surface flow rate in excess of the diverted water, is discharged (exclusively in high-flow seasons) to the San Francisco Bay through the Delta.

3 Methodology

Our methodology involves numerical modeling experiments that use a coupled surface-groundwater hydrologic model that simulates surface hydrology and groundwater dynamics. Figure 2 shows the flowchart we followed in our modeling approach. The flowchart has five key steps. The first step is identifying potential MAR sites - this involves identifying suitable MAR

(recharge) sites based on soil properties and identifying locations on the stream where stream flow can be diverted toward the recharge sites. The second step considers different water diversion rules (i.e. maximum amount of water that can be diverted from the streams to the MAR sites). The third step is numerical modeling experiments conducted using CDWR's C2VSIM model with the identified suitable MAR sites, diversion locations on the streams, and diversion rules identified in previous steps. The fourth step is analysis of model simulations focusing on the following: (i) groundwater recovery, (ii) changes in water balance, and (iii) low-flow augmentation and flood-risk reduction. In the following sections, we discuss each of these steps in further detail.

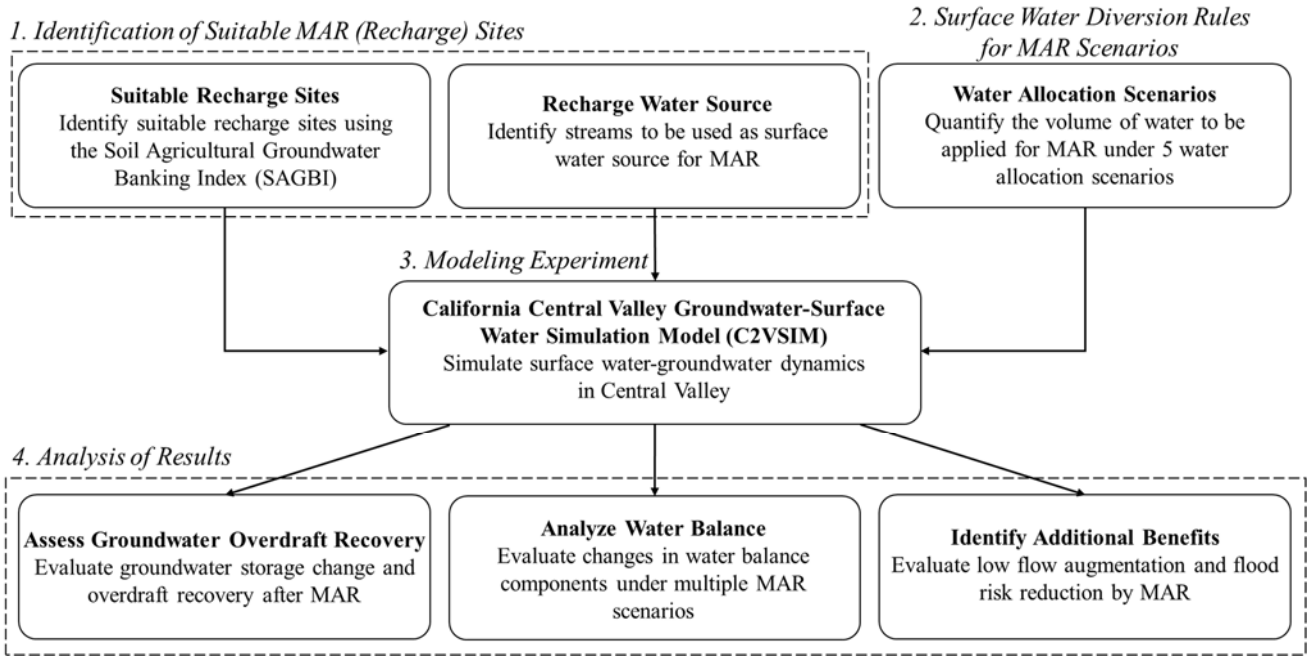

Figure 2. The flowchart used in our modeling experiment.

3.1 Identification of suitable MAR (recharge) sites

We identified suitable recharge sites within each subregion using a two-step process. First, we identified potential sites suitable for recharge based on soil properties - this step classified the

164 land into MAR-suitable and MAR-unsuitable areas. Then, we identified locations on the stream
165 within each of the 21 CDWR subregions (we considered subregions without any stream to be
166 MAR-unsuitable regardless of suitability based on soil properties). In addition, this step is
167 helpful in quantifying the amount of water that runs through the stream in each subregion, as this
168 determines the volume of water that can be diverted –(subregions that have multiple
169 streams/rivers flowing through them could get water from multiple streams for MAR in contrast
170 with subregions with a single stream/river).

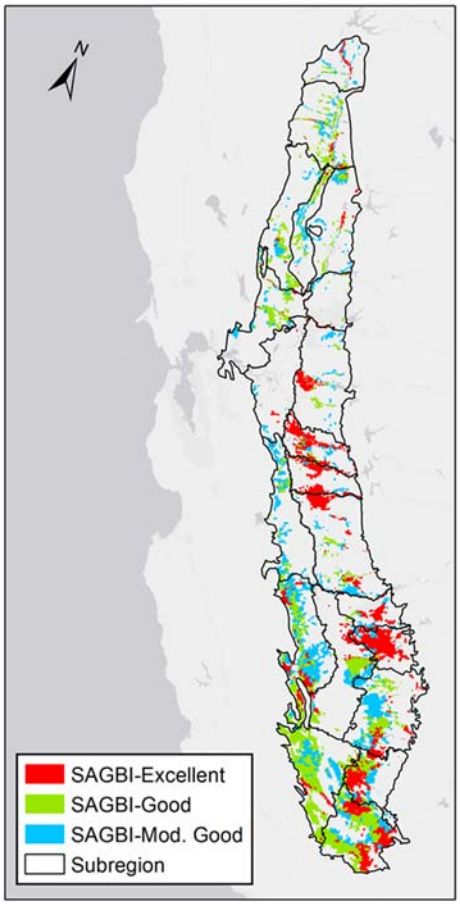

171

172 **Figure 3.** SAGBI classified excellent, good, and moderately good recharge sites in CV.

As discussed above, the first step is identifying potentially suitable sites based on their soil properties. The physical and geological characteristics of a recharge site determine the efficiency of groundwater overdraft recovery by MAR (Ghasemizade et al., 2019). Recharge sites that consist of relatively coarse-grained soils (e.g. sand and gravel) have higher recharge rates compared to sites with fine grained soils (e.g., clay). However, the geologic formation of aquifers is heterogeneous where vertical soil column can have multiple soil types, and the recharge potential relies on the subsurface geologic architecture (Maples et al., 2019; Fogg et al., 1986). Therefore, selection of suitable recharge sites based on physical and geologic characteristics of the entire soil column is critical to the success of MAR implementation.

We used the recharge-potential classification recommended by the Soil Agricultural Banking Index, or SAGBI, that takes into account soil properties (O'Geen et al., 2015). The SAGBI classifies lands within the CV into six groups according to their suitability for MAR: excellent, good, moderately good, moderately poor, poor and very poor. The SAGBI classification is based on the following factors: deep percolation, root zone residence time, chemical limitations, topographic limitations, and surface conditions. We used the unmodified version of the SAGBI (O'Geen et al., 2015) that considers the soil permeability derived from the USDA-NRCS Soil Survey Geographic Database (SSURGO) and ignores the effect of agricultural tillage. Since the focus of our study is to test the full potential (i.e. maximum) of MAR for groundwater overdraft recovery, we only considered locations with excellent, good, and moderately good soil suitability as potential recharge sites (see Figure 3).

Given the purpose of our study, we assumed that all the recharge sites within a given subregion would be uniformly recharged, provided that there is at least one stream crossing the region (more discussion below), however, in reality, the depth of water that can be applied to a recharge

196 site may be limited by additional factors, such as the height of berms or the depth of recharge
197 basins, conveyance structure capacity from hydraulic engineering perspective, and crop
198 sensitivity to stagnant water (for agricultural lands).

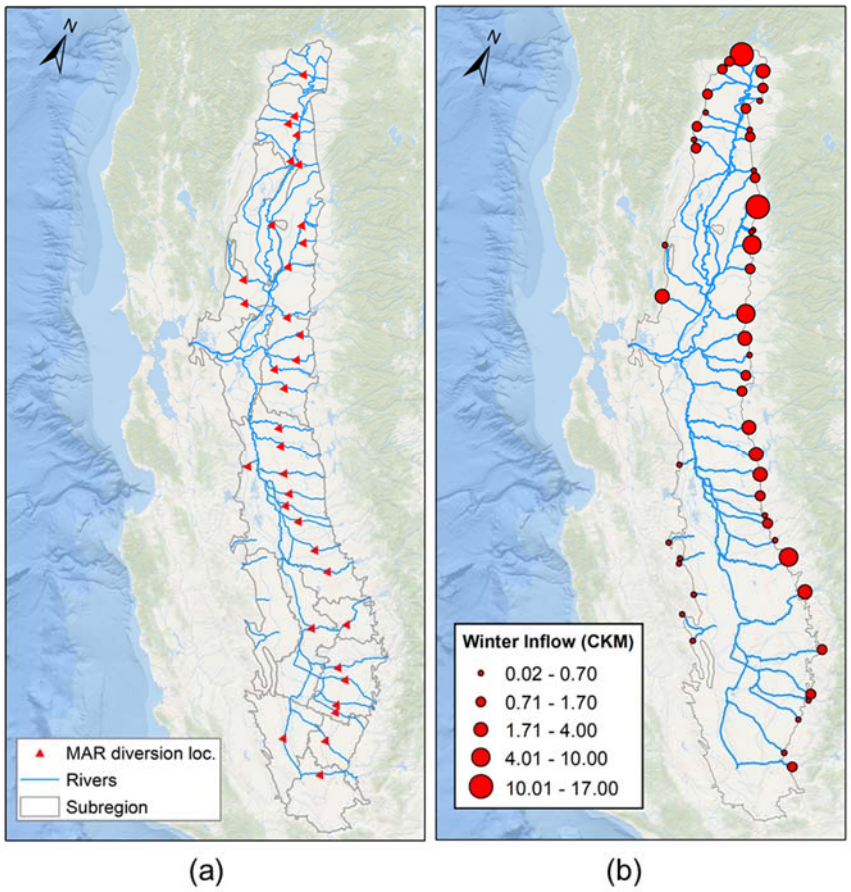

199

200 **Figure 4.** (a) Surface water diversion location for MAR. (b) November-March headwater
201 watershed inflow exceeding the 90th percentile in km^3/year for the period 1960-2015.

202 In the CV, the surface water originating from the headwater watersheds flows through
203 interconnected rivers and enters the subregion, serving as the source of recharge water for the
204 subregion. We identified locations on the rivers where recharge water could be diverted to the
205 MAR sites. Depending on the subregion, there could be one, multiple, or zero rivers crossing the
206 subregion (see Table S1 of Supplementary Material, which lists diversion streams for each

subregion). Assuming that all rivers crossing a given subregion could provide recharge water to that subregion, we identified diversion locations on each river in each subregion; i.e. a subregion with one river will have one location, a subregion with two rivers will have two locations, and a subregion with no river will have no locations and is deemed unsuitable for MAR. For our modeling experiments, we had to identify exact diversion locations on the rivers for each subregion. For simplicity, we identified the diversion location that had the minimum distance between the river and the recharge sites (diversion locations shown in Figure 4a).

3.2 Surface water diversion rules for MAR scenarios

In the CV, most of the annual precipitation occurs during winter, therefore surface water availability is also high in this season. Figure 4b shows the annual average streamflow entering the CV from the headwater watersheds during winter. The figure shows that the streamflow volumes are higher in the northern headwater watersheds compared to southern headwater watersheds. Once this streamflow enters the CV, the water flows through connected rivers shown in Figure 4b, where it is diverted for agricultural and municipal purposes; the remaining water finally drains to the Delta. During 1960-2015, the average volume of winter Delta outflow was about 18 km^3/year. Delta outflow (on average) increases from December to January and then remains stable up to March. There must be a minimum flow into the Delta to meet environmental and legal requirements. Flows above this requirement are referred to as "excess flow" (see Figure S1 of Supplementary Material for Delta outflow variability).

Surface water diversion rules for MAR depend on two factors: (1) streamflow requirements to meet environmental and legal restrictions in the streams and the Delta, and (2) allowable depth of

water at the recharge sites that can realistically be retained for recharge and would not affect production of winter crops if land is used for agricultural purposes.

Regarding the first factor, presently, no fixed rule is available to define how much excess flow may be diverted for MAR without causing environmental conflicts. However, there is a general consensus that streamflow above the 90th percentile threshold (during the period November to March) could be considered for allocation for MAR (Olden & Poff, 2003; Baker et al., 2004; USGS, 2016, Kocis & Dahlke, 2017). Therefore, we calculated the 90th percentile of winter flow at each diversion location (shown in Figure 4a) and considered winter flows that exceeded the 90th percentile threshold for application in corresponding subregions for MAR (referred to as the R90 scenario). Additionally, we tested a less restrictive threshold, the 80th percentile (R80 scenario) as well. In reality, the volume of water that can actually be applied depends on the existence of a conveyance system and its capacity to carry water to the recharge sites. Here, we assume that the allocated volume of water could be delivered to the MAR sites (i.e., was not constrained by the conveyance system).

Regarding the second factor, MAR can negatively affect winter crops in the recharge sites if the sites are agricultural land and water is stagnant for longer period. On average, the maximum depth of water we considered for MAR is 0.15 m (or about 6 inches) per day or 15 m (or about 180 inches) per month (assuming 30 days per month). Earlier studies of MAR application in the southern CV considered water application depths ranging from 0.61m (about 2 ft) to 3.05 m (about 10 ft) (Kourakos et al., 2019). To consider the maximum allowable depth of MAR application into our scenario experiments, we tested two maximum depths: 0.61 m and 3.05 m. In each of these scenarios, we applied water uniformly to all recharge sites.

In summary, we considered four diversion rules:

- 90th percentile threshold with 2-ft application depth (R90_2ft)
- 90th percentile threshold with 10-ft application depth (R90_10ft)
- 80th percentile threshold with 2-ft application depth (R80_2ft)
- 80th percentile threshold with 10-ft application depth (R80_10ft)

Table 1 shows the annual average water diversions for MAR during 1960-2015 for each major region (MAR allocation for each subregion is presented in Table S2 of Supplementary Material). The diversion volumes are higher in the north, due to higher excess water availability. In contrast, the diversion volumes in the south are less variable due to relatively low winter inflows. The calculated total target volumes are 1.4 km^3/year (R90_2ft), 2.32 km^3/year (R80_2ft), 2.65 km^3/year (R90_10ft) and 4.50 km^3/year (R80_10ft), respectively, during 1960-2015. MAR allocation in SC, EZ, SJ, and TL are on average 60%, 19%, 10% and 11% of the total water allocated. In situations where diversion volume is higher than the available streamflow, C2VSIM adjusts the diversion volume for MAR.

Table 1. Water diversions by regions (in km^3/yr) for MAR under different scenarios. Here, SC, EZ, SJ, TL and CV represent Sacramento (SC), East-Delta (EZ), San Joaquin (SJ), Tulare (TL) and Central Valley (CV) respectively.

Scenarios	SC	EZ	SJ	TL	CV
R90_2ft (km^3/yr)	0.85	0.16	0.18	0.20	1.40
R80_2ft (km^3/yr)	1.44	0.26	0.32	0.30	2.32
R90_10ft (km^3/yr)	1.85	0.38	0.22	0.21	2.65
R80_10ft (km^3/yr)	3.17	0.61	0.42	0.30	4.50

In the above scenarios, streams (originating from headwater watersheds) crossing each sub-region are considered "source" water for MAR in each sub-region. Due to the spatial variability

of rainfall (see Figure 1d), subregions in the northern part are expected to receive more recharge water compared to subregions in the southern part. Similarly, northern regions contribute more excess Delta flow than the southern regions. We added one additional scenario, where the streamflow in the Delta that exceeded the 90th percentile threshold and exceeded the 2-ft application depth was transferred to the southern subregions in the SJ and TL basins. In this scenario, we kept the maximum application depth of recharge water as 2 ft in SJ and TL. We labelled this scenario as "R90_2ft_WT".

A critical issue related to water transfer for MAR is the existence of conveyance facilities. In CV, Delta water is already transferred to the south in practice, via aqueducts hundreds of miles long (most of this transfer occurs during the growing season). The difference in water demand-supply balance between the northern and southern CV motivated the construction of the Central Valley Project (CVP) and State Water Project (SWP) aqueducts, precisely for the prupose of transferring water from the Delta to the south. However, it is not presently known whether these aqueducts could be used to transfer excess water for MAR due to capacity and legal issues. In our case, we assumed that the existing infrastructure is capable of transferring water to the south (SJ and TL) for MAR.

3.3 Model description

We used the California Central Valley Simulation Model (C2VSIM), developed and maintained by CDWR. We chose this model for a number of reasons. First, this model was developed, calibrated, and validated for the CV, and takes into account the main hydrological processes in the region. Second, the use of this model facilitates the communication and transfer of results to

CDWR. CDWR has made Flood-MAR a priority and is soliciting inputs from the community - an example is the 2019 Flood-MAR Public Forum organized by CDWR in October 2019.

C2VSIM is an integrated surface and groundwater model that is capable of simulating hydrologic processes including surface runoff, streamflow, land surface, and root zone processes, the vadose zone, and saturated groundwater flow (Brush et al. 2013). There are two versions of C2VSIM available based on the resolution of finite elements, coarse-grid (C2VSIM-CG) and fine-grid (C2VSIM-FG), the latter of which is used for this study (hereafter, C2VSIM-FG is referred as C2VSIM). C2VSIM was calibrated by Brush et al. (2013) and applied in multiple previous studies in the region (e.g., Alam et al., 2019; Kourakos et al., 2019; Ghasemizade et al., 2019; Dogrul et al. 2016).

The model dynamically calculates the agricultural and urban water demand, links these to groundwater pumping and surface water diversions, and adjusts water deliveries based on demands. C2VSIM requires user-inputs for precipitation, evapotranspiration, irrigation method, crop distribution, population, boundary inflow, and surface water delivery. The model calculates the surface runoff, return flow, infiltration and vertical movement of soil moisture in the root zone, and aquifer recharge. The amount of crop water demand unmet by surface water and root zone soil moisture is dynamically supplemented from groundwater pumping. Crop water demand is calculated based on crop evapotranspiration rates, irrigation efficiency, stream diversion, precipitation, and crop distribution.

Figure 5 shows the major processes considered by C2VSIM. C2VSIM uses three vertical layers. The top layer represents the unconfined aquifer and the bottom two layers represent confined aquifers. The confined and unconfined aquifers are separated by a thin layer of Corcoran clay.

Horizontally, the region is divided into finite element computational polygons, which have irregular shapes. Each corner of finite element is called a groundwater node. C2VSIM uses the Galerkin finite element method to solve the governing equation at each groundwater node. Stream connectivity in C2VSIM is defined by a series of inflow and outflow nodes, which represent the locations where water is received from surface runoff, return flow and other nodes, and where the water is diverted for irrigation and other downstream nodes. Stream-aquifer interactions depend on the head gradient between the stream stage and groundwater head and streambed conductance.

The model operates at a monthly time step. We used the baseline period 1960-2015 (water years). Therefore, our analyses are derived from 56 years of historical data (inputs) and corresponding monthly simulations.

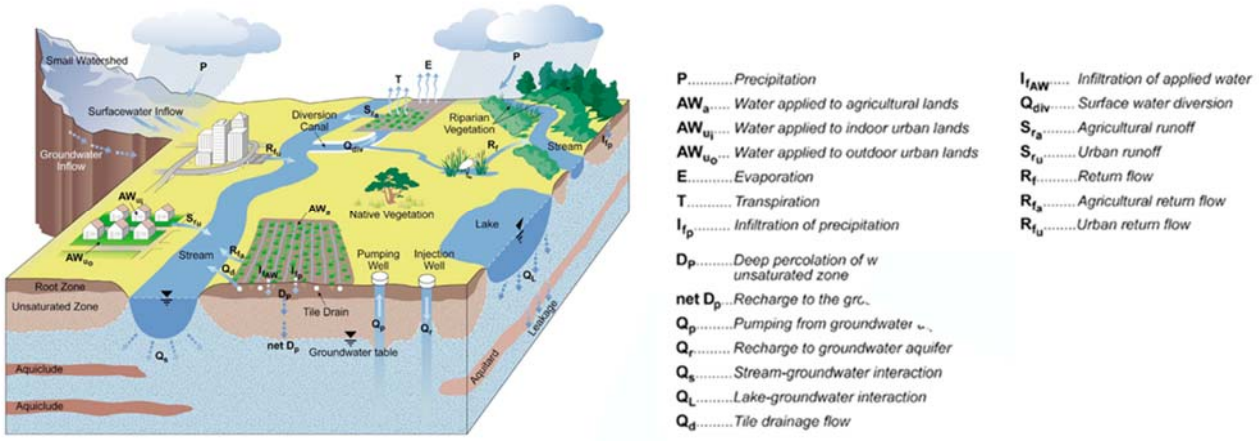

Figure 5. Major hydrologic processes modeled by the C2VSIM (IWFM manual)

4 Results and discussion

4.1 Groundwater storage change

4.1.1 Baseline groundwater storage change during 1960-2015

First, we quantified the groundwater storage change between the end-years of the baseline period, 1960 and 2015, for each of the subregions (Figure. 6a). The change in groundwater storage varies within the region. In general, the southern region (almost half of the CV) has the most serious groundwater overdraft problem, while the northern region has exhibited little to no change in groundwater storage in recent decades. The groundwater overdraft in the southern CV is severe: the largest overdraft is 0.71 km^3/yr and takes place in SR-18 in the TL. The next largest overdrafts are between 0.41 km^3/yr and 0.40 km^3/yr and take place in SR-10 (SJ basin) and SR 17 (TL basin). The north-south gradient in groundwater overdraft is due to increasing differences in surface water supply and agricultural water demand towards south, which has been met by groundwater pumping. On average, CV groundwater storage has decreased by about 3.1 km^3/year during 1960-2015.

4.1.2 Impact of MAR on groundwater storage change in subregions

We evaluated the groundwater overdraft recovery for the R90 (R90_2ft and R90_10ft) and R80 (R80_2ft and R80_10ft) MAR scenarios. Figure 6b shows the groundwater storage change under R90_2ft scenario, where the spatial distribution of overdraft is quite similar to the base simulation (Figure 6a). The spatial distribution of groundwater storage change for other MAR scenarios have similar patterns, so we only plotted one scenario to show relative magnitudes (Figure 6b). We found that the groundwater storage change under R90_2ft, R90_10ft, R80_2ft and R80_10ft scenarios was -2.8 km^3/year, -2.6 km^3/year, -2.6 km^3/year and -2.4 km^3/year respectively. We also calculated the groundwater overdraft recovery by MAR for each subregion using Equation (1),

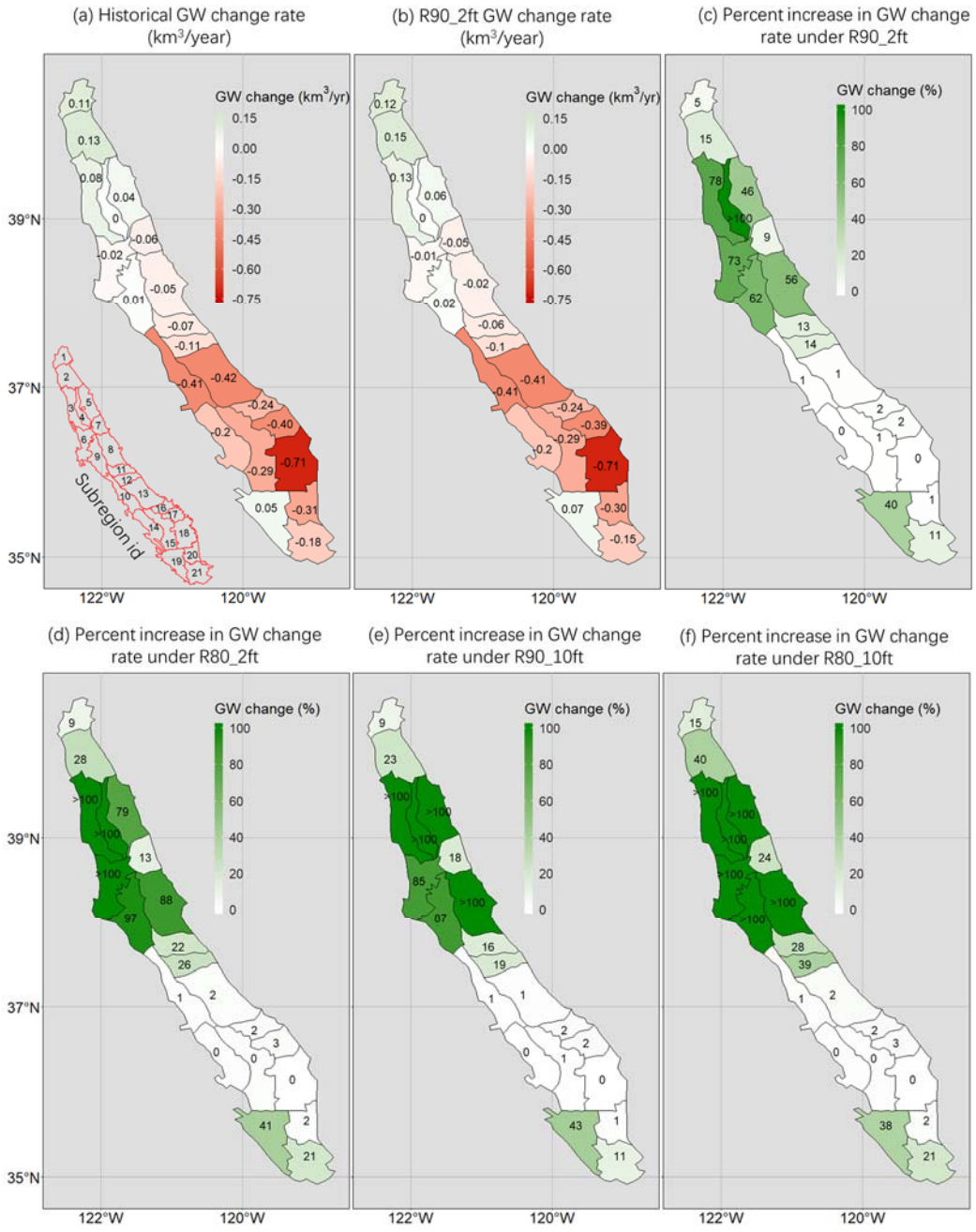

Figure 6. (a) Groundwater storage change rate (km^3/year) in base period (1960-2015), where the unit km^3/year represents the annual average groundwater change in a subregion. The inset shows subregion IDs; (b) R90_2ft groundwater storage change rate (km^3/year); (c-f) Increase in groundwater storage (%) compared to base condition for R90_2ft, R80_2ft, R90_10ft and R80_10ft scenarios respectively.

$$\mathrm{GWC}(\%) = \frac{\sum_{i=1}^{N} \Delta GW_{i,MAR} - \sum_{i=1}^{N} \Delta GW_{i,base}}{\sum_{i=1}^{N} \Delta GW_{base}} \times 100 \quad (1)$$

where, GWC represents the groundwater storage change in percentage after MAR application compared to the base condition. The term GWC also represents groundwater overdraft recovery (%) when there is an overdraft in the base simulation. ΔGW_i represents groundwater change in a given month i compared to previous month. N is total number of months (N=672 months in our case).

Figure 6c-f shows GWC under R90_2ft, R90_10ft, R80_2ft, and R80_10ft scenarios. In SC_EZ (combination of SC and EZ), subregions 2 to 8 show higher GWC, this is due to a higher amount of water application compared to relatively small current groundwater overdraft. Results from the base scenario show that only SR6, SR7 and SR8 have existing groundwater overdraft (Figure 6a) in SC_EZ. MAR would mitigate more than half of the existing groundwater overdraft in SR6 (GWC 73%-100%) and SR8 (GWC 56%-100%), and up to 25% in SR7. The rate of groundwater overdraft recovery is low in SJ and TL subregions, aside from SR11 and SR12 which show higher recovery. The low percentages in Figure 6c-f for most of the SJ and TL subregions are due to low net groundwater recharge compared to relatively high existing overdraft. In TL, only SR19 shows high (compared to the rest of the domain) GWC, which is due to relatively low groundwater storage change in the base scenario compared to other TL subregions in TL.

4.1.3 Impact of MAR on groundwater storage change in major hydrologic regions

Figure 7a shows the percent groundwater overdraft recovery in each of the major hydrologic regions (HR) (see Figure S2 in Supplementary Material for cumulative difference in groundwater storage between MAR and base scenarios). Groundwater overdraft recovery is calculated using

Equation (1). We find MAR can recover 8.9% and 14.1% of the CV's total groundwater overdraft under R90_2ft and R80_2ft scenarios respectively. The recoveries under R90_10ft and R80_10ft are 14% and 22.2%. Groundwater overdraft recovery is highest in SC_EZ, ranging from 27.5% to 57.3% under R90 scenarios (R90_2ft and R90_10ft) and, 56% to 101% under R80 scenarios (R80_2ft and R80_10ft). The relatively high recoveries in SC_EZ are attributable to higher availability of excess surface flow. In SJ, the recoveries range between 3.2% to 7.8%. Recoveries are even lower in TL, where only 2.7% to 3.3% of the existing overdraft can be recovered by any scenario. Low groundwater recovery in SJ and TL is due to low water availability combined with very high existing overdraft. It appears that MAR could effectively recover most of the existing overdraft in SC and EZ, however, SJ and TL will require measure in addition to MAR to mitigate the existing overdraft. Some of the potential measures to reduce overdraft in SJ and TL could include reducing agricultural demand (through land use and cropping pattern and policy changes) and increasing water use efficiency.

4.1.4 Groundwater storage change under water transfer scenario R90_2ft_WT

We quantify the volume of water leaving the Delta above the 90th percentile (excess flow) after implementing the regionwide R90_2ft scenario, which is around 2.2 km^3/year (see Figure S3 of Supplementary Material for cumulative difference in Delta outflow between MAR and base scenarios). This volume of water is the amount that would leave the Delta as excess flow even after applying MAR (R90_2ft scenario). As described in section 3.2, this excess flow could be exported to SJ and TL for MAR application (in the R90_2ft_WT scenario). Figure 7b compares the groundwater overdraft recovery percentage between water transfer scenario R90_2ft_WT and non-water transfer scenario R90_2ft. We find that the R90_2ft_WT scenario significantly

increases groundwater overdraft recovery in SJ and TL, specifically the percent of overdraft recovery increased to 63%, 62% and 30% from 9%, 3% and 3% in CV, TL and SJ respectively.

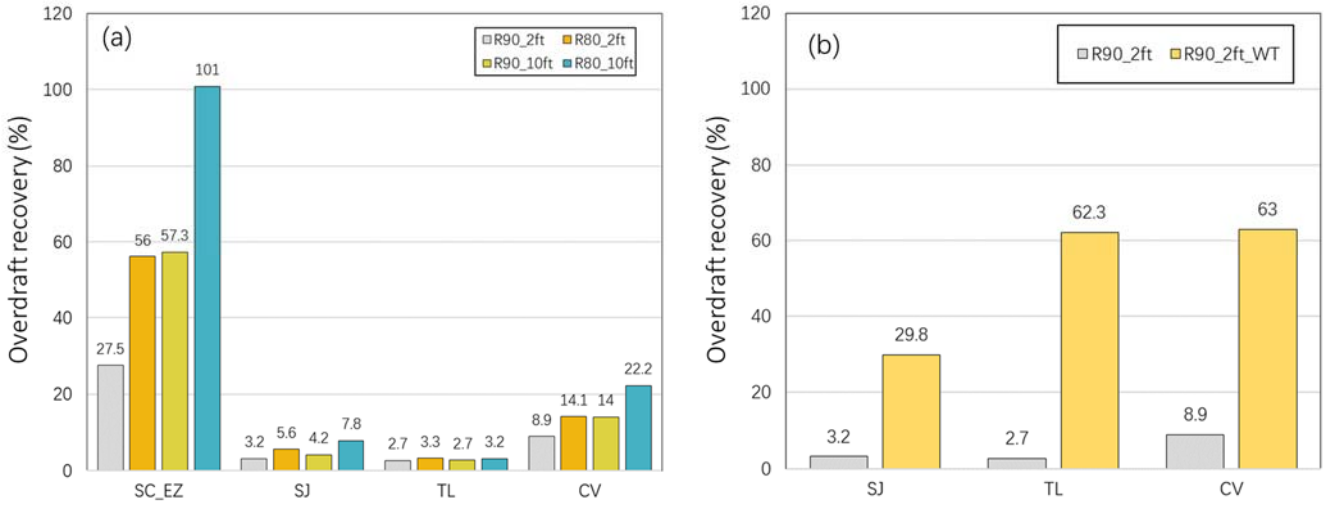

Figure 7. Percent groundwater overdraft recovery under (a) R90_2ft, R80_2ft, R90_10ft and R80_10ft scenarios, and (b) R90_2ft and Delta export scenario (R90_2ft_WT).

4.2 Changes in groundwater balance components

Groundwater storage change in an aquifer is the result of a balance among recharge, stream-aquifer interaction, return flow, net subsurface flow, groundwater pumping, and deep percolation. These groundwater balance components are expected to vary among regions. Here, we calculate the cumulative difference in each of the groundwater balance components between MAR and the base scenario using equation (2).

$$\text{Cumulative change} = \frac{\sum_{i=1}^{N} Var_{i,MAR} - \sum_{i=1}^{N} Var_{i,base}}{Total\ years} \quad (2)$$

Where, VAR_i represents water balance component for month i. Total years considered are 56 (1960-2015). The unit of cumulative change is in km^3/year.

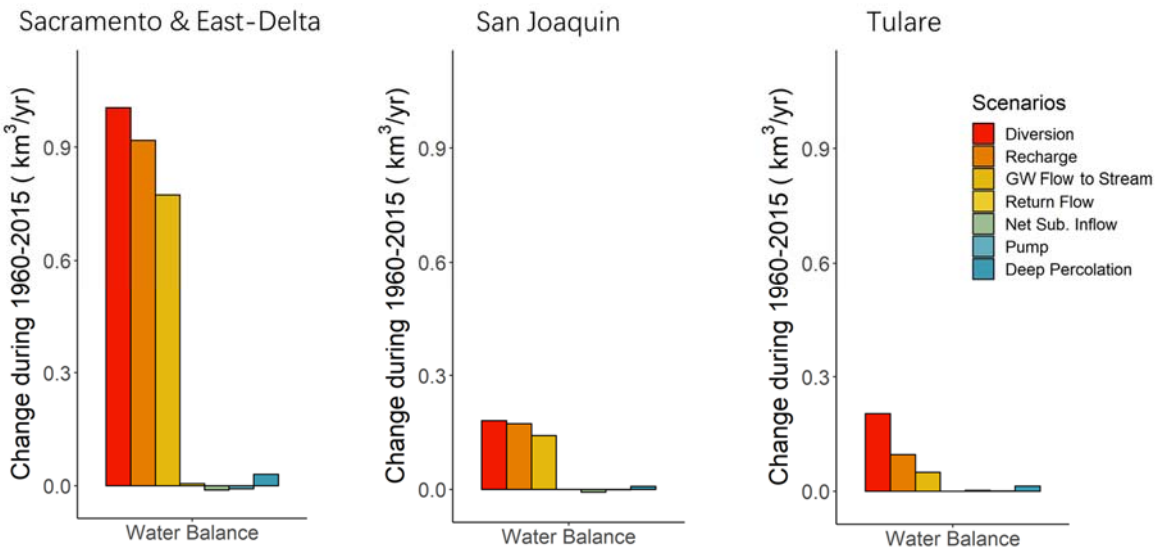

412

413 **Figure 8.** Change in water balance components for R90 scenario compared to base condition
414 averaged over 1960-2015. The water balance components shown here include diversions for
415 MAR, recharge, lateral flow from groundwater flow to stream, net subsurface inflow from
416 neighboring subregions (Net Sub. Inflow), pumping, and deep percolation.

417 Figure 8 shows the cumulative change in water balance components (per year) relative to the
418 base condition in the major regions (SC, EZ, SJ, and TL) of CV under the R90_2ft scenario. We
419 show the comparison for R90_2ft only because it is representative of the relative contribution of
420 each of the water balance components. Figure 8 shows that the water allocation (or diversion) for
421 MAR is higher in SC_EZ compared to SJ and TL, which is due to higher surface water
422 availability in SC_EZ. As surface water diversions to MAR sites increase, groundwater recharge
423 also increases in all regions, with a relatively higher rate in SC_EZ and SJ (see Figure S4 of
424 Supplementary Material for cumulative difference in recharge between MAR and base
425 scenarios). The increase in groundwater recharge also increases lateral flows from groundwater
426 to stream (we discuss this in the next section). Furthermore, we find that the effect of MAR is not

427 significant on other water balance components, e.g. return flow, net subsurface inflow, pumping,
428 and deep percolation.

429 4.3 Changes in stream-aquifer interaction

430 The net volume of groundwater overdraft recovery is influenced by stream-aquifer interactions.
431 Two factors are important in defining the direction and volume of subsurface flows: (1)
432 horizontal hydraulic conductivity; and (2) head difference between the groundwater table and the
433 connected stream. Higher hydraulic conductivity results in relatively fast movement of
434 subsurface water, whereas greater positive head differences (difference between the groundwater
435 table and stream water level) results in greater movement of water from the aquifer to the stream.
436 In our simulations, all regions showed increased flow from the aquifer to the stream (Figure 8)
437 with MAR. To better demonstrate how stream-aquifer interactions vary between regions and
438 over time, we calculated cumulative stream-aquifer interactions using equation (2) for major
439 regions.

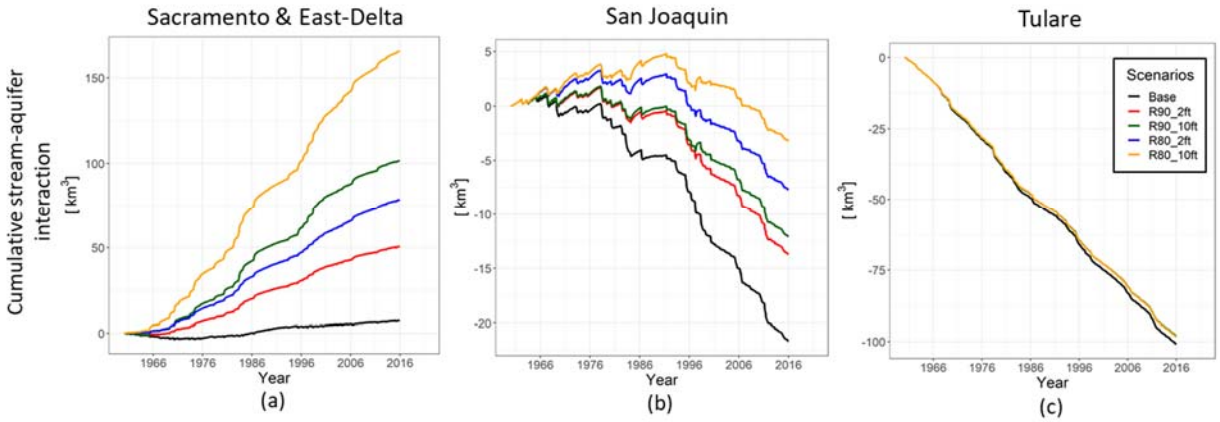

440

441 **Figure 9.** Cumulative stream aquifer interactions in SC_EZ (left), SJ (middle) and TL (right) for
442 the base and MAR scenarios. A positive value indicates flow from groundwater to stream, a
443 negative value indicates vice versa.

444 Figure 9 shows the cumulative stream-aquifer interaction in SC_EZ, SJ, and TL during 1960-
445 2015. The increase in groundwater recharge (as shown in Figure 8) associated with MAR raises
446 the groundwater table relative to the base scenario, thereby changing the relative head difference
447 between surface water and groundwater table. This changes the stream-aquifer dynamics
448 compared to the base scenario. In SC_EZ, the cumulative stream-aquifer interaction is close to 0
449 for the base condition, which shows a positive trend in MAR scenarios due to increased
450 groundwater flow from the aquifer to stream. This shows that a fraction of groundwater recharge
451 by MAR actually returns back to the stream through subsurface flow (or base flow). SJ and TL
452 have different situations as shown in Figure 9. In both SJ and TL, cumulative stream-aquifer
453 interactions are negative during the base scenario, which indicates that the groundwater table is
454 lower than stream water level and there is a net flow from stream to the aquifer in the base
455 condition. As MAR is implemented, the groundwater table rises and the hydraulic head
456 difference between stream and aquifer is changed; this results in modified flow between stream-
457 aquifer compared to the base case. In SJ, the cumulative stream-aquifer exchange is relatively
458 stable from about 1960-1978 as in the base condition, when MAR would have resulted in net
459 flow from the aquifer to the stream. However, due to intensive groundwater extraction in SJ in
460 the later part of the simulation period, the groundwater table dropped substantially and resulted
461 in net negative stream-aquifer interactions even with the implementation of MAR. In TL, the
462 aquifer was overexploited throughout the base period, therefore the groundwater table was much
463 lower than the stream and the cumulative stream-aquifer interaction was always negative (Figure
464 9c). With MAR, there is a slight positive impact as seen is Figure 9c, but it is not large due to the
465 limited water volume available for Figure 9 shows the cumulative stream-aquifer interaction in
466 SC_EZ, SJ, and TL during 1960-2015. The increase in groundwater recharge (as shown in

Figure 8) associated with MAR raises the groundwater table relative to the base scenario, and alters the relative head difference between surface water and groundwater table, resulting in changes in the stream-aquifer dynamics compared to the base scenario. In SC_EZ, the cumulative stream-aquifer interaction is close to 0 for the base condition, but MAR scenarios exhibit positive trend due to the recharge. This indicates that a fraction of groundwater recharge by MAR actually returns back to the stream through subsurface flow (or base flow). SJ and TL have different situations as shown in Figure 9. In both SJ and TL, cumulative stream-aquifer interactions are negative during the base scenario, which indicates that the groundwater table is lower than stream water level and there is a net flow from stream to the aquifer in the base condition. As MAR is implemented, the groundwater table rises and the hydraulic gradient between stream and aquifer is changed compared to the base case. In SJ, cumulative stream-aquifer exchange is relatively stable and balanced during 1960-1978 in the base condition, but off balance afterwards when intensive groundwater extraction accelerates the aquifer depletion in SJ. The MAR implementation will alleviate the groundwater depletion trend under all scenarios. In TL, the stream-aquifer interaction appears to be insensitive to the MAR, indicating that the aquifer is essentially disconnected from the stream due to the severe overexploitation (Winter et al., 1998).

4.4 Role of MAR in low flow augmentation

Summertime (July-September) low flow is an important source of water for fisheries and ecosystem functioning. Lateral groundwater flow (baseflow) from aquifers is an important (often primary) source of summertime low flow. Baseflow generally occurs due to the head difference between groundwater and surface water, where higher (positive) head differences lead to greater baseflow. MAR enhances base flow by increasing net groundwater storage in the aquifers, which

can play a vital role during water-scarce drought years. MAR's ability to enhance low flows varies between regions due to variations in soil characteristics (e.g. horizontal and vertical hydraulic conductivity). We analyzed the baseflow change after MAR implementation for our entire simulation period (1960-2015), and separately for the 2007-2009 drought and 2012-2015 drought periods.

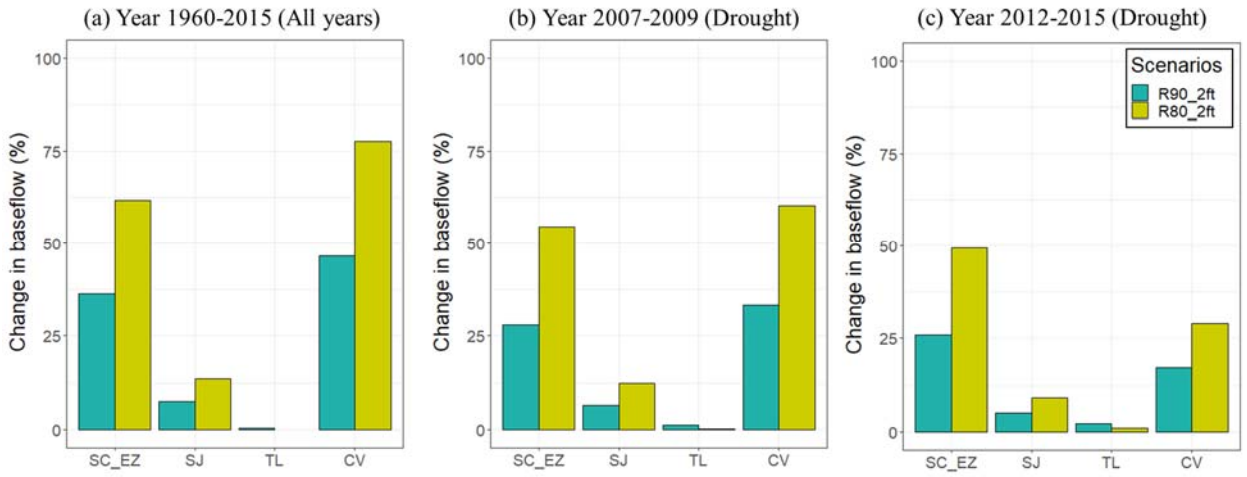

Figure 10. Summertime (July-September) baseflow changes during the entire study period 1960-2015 (left), the 2007-2009 drought (middle) and the 2012-2015 drought (right).

Figures 10a-c show the percent changes in baseflow for the entire simulation period and for the two drought periods only. The figures show that there is a net increase in baseflow during 1960-2015 in CV of about 47% and 78% for R90_2ft and R80_2ft scenarios respectively (Figure 10a). The northern region (SC and EZ) generally has the greatest increases in baseflow, which can be explained by greater water allocation (for MAR) leading to higher groundwater head differences between stream and aquifer. Baseflow increased by about 37% and 62% in SC_EZ and, 7% and 13% in SJ for R90_2ft and R80_2ft scenarios respectively during 1960-2015 (Figure 10a). In TL, the baseflow increases are relatively small (~1%). The changes in baseflow during summer

months after MAR implementation is promising, as they undoubtedly would promote environmental and ecological sustainability. We also computed the baseflow changes under R90_10ft and R80_10ft scenarios (not shown in Figure 10). Baseflow increased by about 85% and 146% in SC_EZ and, 9% and 18% in SJ for R90_10ft and R80_10ft scenarios respectively during 1960-2015. In all cases, cases baseflow increase in TL is lower than other major regions. The varying effects of MAR on the baseline has been discussed in the last section on stream-aquifer interaction.

MAR is intended to promote drought resilience in the CV through groundwater banking in the wet years. To evaluate the extent to which this would be the case, we compared baseflow changes during the 2007-2009 and 2012-2015 droughts. Figures 10b-c show the percent changes in baseflow during the 2007-2009 and 2012-2015 droughts, respectively. The baseflow increase due to MAR is substantial in most of the subregions during the drought years. We find that MAR would increase baseflow over the entire CV during the 2007-2009 drought by around 28% (R90_2ft) and 60% (R80_2ft) and, around 17% and 29% during 2012-2015 under the R90_2ft and R80_2ft scenarios respectively. The baseflow increase is higher in SC, where almost all regions show enhanced baseflow. The magnitude of base flow increase is related to the volume of water applied for MAR. Most of the subregions in SJ and TL also show increased baseflow during the drought, with the greatest increase in SR10-SR12 and SR16. Overall, MAR increases summertime low flows, especially during drought periods, by as much as 52% (with no redistribution of excess flows) and 73% if excess flows are redistributed from north to south. This finding confirms that MAR could enhance drought resilience and promote environmental sustainability in the CV.

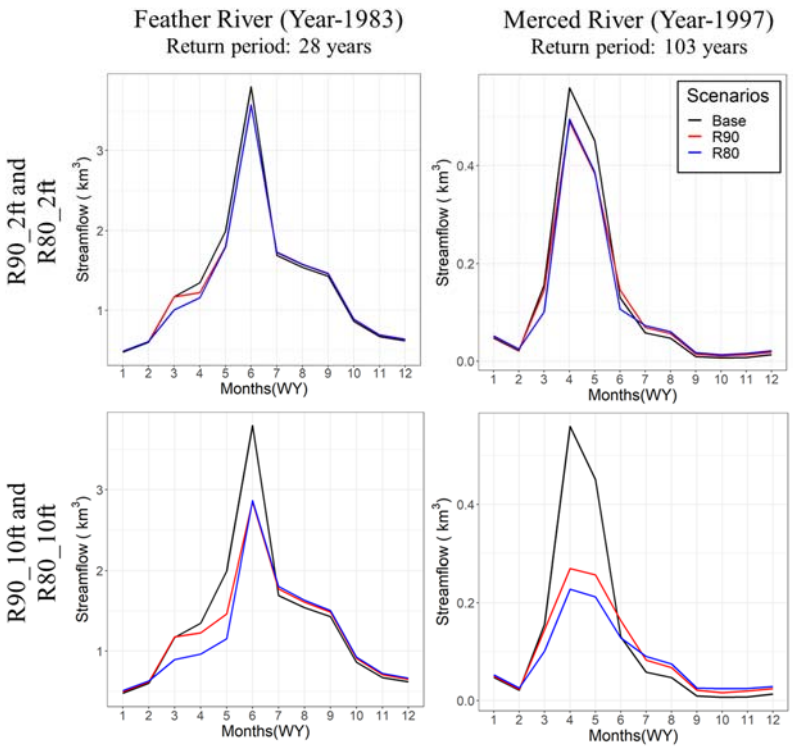

528

529 **Figure 11.** Monthly hydrograph for two wet years (1983 and 1997) near the outlets of Feather
530 River (top row) and Merced River (bottom row). In all the plots, the black line represents the
531 base simulation, and the red and blue lines in the top row represent R90_2ft and R80_2ft
532 scenarios respectively, and the 10 ft recharge scenarios (R90_10ft and R80_10ft respectively) in
533 the bottom row.

534 4.5 Role of MAR in flood risk reduction

535 MAR would divert high flows from the streams, hence resulting in flood peak reduction. Figure
536 11 shows the monthly hydrograph of the Feather River for 1983 and the Merced River for 1997 –
537 two years with major floods in these two headwater basins. The peak discharge in both basins
538 usually occurs between January to March. We find that the peak discharge decreases in all cases
539 with MAR implementation, with higher depletions when more water is diverted. The comparison

between scenarios with different maximum depth (2ft and 10ft), show that much greater reductions in flood peak occur when the maximum allowable depth is increased from 2ft to 10ft (Figure 11) especially in the extreme (estimated return period 103 years) Merced River flood of 1997. Overall, we find peak flow decreased by around 10%-40% (during February-March) in Feather River and 12%-59% (during January-February) in Merced River.

5. Summary and Conclusions

Groundwater plays a vital role in the Central Valley's water supply, especially during drought periods. Over our 56-year study period (1960-2015), groundwater storage in the CV has progressively decreased by an average of around 3 km^3/year. MAR has the potential to replenish groundwater through the application of high winter flows to agricultural lands and would act as a groundwater bank. Our objective was to quantify the groundwater overdraft recovery that would be possible through regionwide application of MAR and to quantify other ancillary benefits. We conducted numerical experiments using a surface-groundwater hydrological model where winter flows exceeding the 90th (R90 scenario) and 80th (R80 scenario) percentiles were assumed to be applied for MAR. Based on our simulations, we conclude that:

- MAR could potentially recover 9 - 22% (for R90 and R80 scenarios, respectively) of the existing groundwater overdraft aggregated over the entire CV. The effect of MAR varies among regions. In northern CV (i.e. Sacramento) where groundwater depletion is not a major problem (compared to southern CV), the effect of MAR is high. In southern CV (i.e. San Joaquin and Tulare) where groundwater overdraft is large, MAR cannot solve the problem. We find that the contribution of MAR to the reduction of the historic groundwater overdraft would be about 3- 8% in the San Joaquin (SJ) region, and even

562 less (about 3%) in the Tulare (TL) region. The primary cause of low groundwater
563 recovery in the southern CV (SJ and TL regions) is the lack of adequate headwater
564 supply in relation to the large existing groundwater overdraft.

565 • The application of MAR using streamflow crossing each region cannot solve the
566 groundwater overdraft problem in the southern CV. However, a larger portion of the
567 groundwater overdraft problem in SJ and TL could be mitigated through the delivery of
568 excess winter flow from northern CV to southern CV for MAR. We investigated the
569 effect of delivering excess winter delta outflow (over 90th percentile) to the southern CV
570 for MAR, this would increase CV-wide groundwater overdraft recovery to 63%, and 30%
571 in SJ and 62% in TL.

572 • The application of MAR would have ancillary benefits in addition to groundwater
573 overdraft recovery. MAR would augment summertime low flows, especially during
574 drought periods CV-wide by as much as 52% (with no redistribution of excess flows) and
575 73% if excess flows were redistributed from north to south. Moreover, we tested the
576 effect of MAR on streamflow of Feather River and Merced River during two large flood
577 events (year-1983 and year-1997), where it effectively reduces the flood peaks by 10%-
578 40% in Feather River and 12%-59% in Merced River.

579 **Acknowledgements:**

580 All data used in this research are publicly available. C2VSIM fine grid version is publicly
581 available online: https://data.cnra.ca.gov/dataset/c2vsimfg_beta2 . Anyone interested in SAGBI
582 map can request Dr. O'Geen of Dept. of Land, Air and Water Resources at University of
583 California, Davis, and the data will be available for the requestor to download. Other

584 representative data in this paper are uploaded to the link
585 https://doi.org/10.6084/m9.figshare.11740050.v3

586 We acknowledge the University of California Research Initiatives Award LFR-18-548316 for
587 supporting this work. We are grateful to Dr. Emin Dogrul and Dr. Tyler Hatch from the
588 California Department of Water Resources for technical assistance in the use of C2VSIM.

589 **References**

590 Alam, S., Gebremichael, M., Li, R., Dozier, J., & Lettenmaier, D. P. (2019). Climate change
591 impacts on groundwater storage in the Central Valley, California. Climatic Change, 157(3-4),
592 387-406.

593 Alley, W. M., Healy, R. W., LaBaugh, J. W., & Reilly, T. E. (2002). Flow and storage in
594 groundwater systems. Science, 296(5575), 1985–1990.

595 Bachand, P. A. M., Roy, S. B., Choperena, J., Cameron, D., & Horwath, W. R. (2014).
596 Implications of using on-farm flood flow capture to recharge groundwater and mitigate flood
597 risks along the Kings River, CA. Environmental Science & Technology, 48(23), 13,601–13,609.
598 https://doi.org/10.1021/es501115c

599 Brown, L. R., Kimmerer, W., & Brown, R. (2009). Managing water to protect fish: a review of
600 California's environmental water account, 2001–2005. Environmental management, 43(2), 357-
601 368.

602 Baker D B, Richards R P, Loftus T T and Kramer J W 2004 A new flashiness index:
603 characteristics and applications to midwestern rivers and streams J. Am. Water Resour. As. 40
604 503–22

Brush, C.F., Dogrul, E.C. and Kadir, T.N., 2013. *Development and calibration of the California Central Valley Groundwater-Surface Water Simulation Model (C2VSim), version 3.02-CG*. Bay-Delta Office, California Department of Water Resources.

California Law (2014). *Sustainable Groundwater Management*. Retrieved from http://leginfo.legislature.ca.gov/faces/codes_displayexpandedbranch.xhtml?tocCode=WAT&division=6.&title=&part=2.74.&chapter=&article

CDWR (2019). *Flood-MAR Research and Data Development Plan*. Retrieved from https://water.ca.gov//media/DWR-Website/Web-Pages/Programs/Flood-Management/Flood-MAR/Flood-MAR-RDD-Plan_a_y_19.pdf

Chinnasamy, P., Muthuwatta, L., Eriyagama, N., Pavelic, P. and Lagudu, S., 2018. Modeling the potential for floodwater recharge to offset groundwater depletion: a case study from the Ramganga basin, India. Sustainable Water Resources Management, 4(2), pp.331-344.

Dahlke, H. E., Brown, A. G., Orloff, S., Putnam, S., & O'Geen, A. (2018). Managed winter flooding of alfalfa recharges groundwater with minimal crop damage. California Agriculture, 72(1), 1–11. https://doi.org/10.3733/ca.2018a0001

Dillon, P., Stuyfzand, P., Grischek, T., Lluria, M., Pyne, R.D.G., Jain, R.C., Bear, J., Schwarz, J., Wang, W., Fernandez, E. and Stefan, C., 2019. Sixty years of global progress in managed aquifer recharge. Hydrogeology journal, 27(1), pp.1-30.

Dogrul, E.C., Kadir, T.N., Brush, C.F. and Chung, F.I., 2016. Linking groundwater simulation and reservoir system analysis models: The case for California's Central Valley. Environmental modelling & software, 77, pp.168-182.

626 Dogrul, E. C., Kadir, T. N., & Brush, C. F. (2017). DWR Technical Memorandum: Theoretical
627 Documentation and User's Manual for IWFM Demand Calculator (IDC-2015), Revision 63,
628 August 2017, Sacramento, 312 pages.

629 Famiglietti, J. S., Lo, M., Ho, S. L., Bethune, J., Anderson, K. J., Syed, T. H., et al. (2011).
630 Satellites measure recent rates of groundwater depletion in California's Central Valley.
631 Geophysical Research Letters, 38, L03403. https://doi.org/10.1029/2010GL046442

632 Fogg, G. E. (1986). Groundwater flow and sand body interconnectedness in a thick, multiple-
633 aquifer system. Water Resources Research, 22(5), 679-694.

634 Ghasemizade, M., Asante, K.O., Petersen, C., Kocis, T., Dahlke, H.E. and Harter, T., 2019. An
635 integrated approach toward sustainability via groundwater banking in the southern Central
636 Valley, California. Water Resources Research, 55(4), pp.2742-2759.

637 Gorelick, S. M., & Zheng, C. M. (2015). Global change and the groundwater management
638 challenge. Water Resources Research, 51, 3031–3051. https://doi.org/10.1002/2014WR016825

639 Hanak, E., Escriva-Bou, A., Gray, B., Green, S., Harter, T., Jezdimirovic, J., Lund, J., Medellín-
640 Azuara, J., Moyle, P. and Seavy, N. (2019). Water and the Future of the San Joaquin
641 Valley. Public Policy Institute of California.

642 Hanson, R. T., Flint, L. E., Flint, A. L., Dettinger, M. D., Faunt, C. C., Cayan, D., & Schmid, W.
643 (2012). A method for physically based model analysis of conjunctive use in response to potential
644 climate changes. Water Resources Research, 48(6).

645 Hashemi, H., Berndtsson, R., & Persson, M. (2015). Artificial recharge by floodwater spreading
646 estimated by water balances and groundwater modelling in arid Iran. Hydrological Sciences
647 Journal, 60(2), 336-350.

648 Kocis, Tiffany N., and Helen E. Dahlke. "Availability of high-magnitude streamflow for
649 groundwater banking in the Central Valley, California." *Environmental Research Letters* 12, no.
650 8 (2017): 084009.

651 Kourakos, G., Dahlke, H.E. and Harter, T., 2019. Increasing Groundwater Availability and
652 Seasonal Baseflow through Agricultural Managed Aquifer Recharge in an Irrigated Basin. Water
653 Resources Research.

654 Li, R., Ou, G., Pun, M., & Larson, L. (2018). Evaluation of Groundwater Resources in Response
655 to Agricultural Management Scenarios in the Central Valley, California. Journal of Water
656 Resources Planning and Management, 144(12), 04018078.

657 Maples, S. R., Fogg, G. E., & Maxwell, R. M. (2019). Modeling managed aquifer recharge
658 processes in a highly heterogeneous, semi-confined aquifer system. Hydrogeology
659 Journal, 27(8), 2869-2888.

660 Niswonger, R.G., Morway, E.D., Triana, E. and Huntington, J.L., 2017. Managed aquifer
661 recharge through off-season irrigation in agricultural regions. Water Resources Research, 53(8),
662 pp.6970-6992.

663 O'Geen, A., Saal, M., Dahlke, H., Doll, D., Elkins, R., Fulton, A., et al. (2015). Soil suitability
664 index identifies potential areas for groundwater banking on agricultural lands. California
665 Agriculture, 69,75–84. https://doi.org/10.3733/ca.v069n02p75

666 Olden J D and Poff N L 2003 Redundancy and the choice of hydrologic indices for
667 characterizing streamflow regimes River Res. Appl. 19 101–121

668 Roddell, M., I. Velicogna, and J.S. Famiglietti 2009. Satellite-based estimates of groundwater
669 depletion in India. Nature, 460 999-1002, doi: 10.1038/nature08238.

670 Ronayne, M. J., Roudebush, J. A., & Stednick, J. D. (2017). Analysis of managed aquifer
671 recharge for retiming streamflow in an alluvial river. Journal of hydrology, 544, 373-382.

672 Scanlon, B. R., Reedy, R. C., Faunt, C. C., Pool, D., & Uhlman, K. (2016). Enhancing drought
673 resilience with conjunctive use and managed aquifer recharge in California and Arizona.
674 Environmental Research Letters, 11(3), 035013.

675 Siebert, S., Burke, J., Faures, J. M., Frenken, K., Hoogeveen, J., Doll, P., & Portmann, F. T.
676 (2010). Groundwater use for irrigation—A global inventory. Hydrology and Earth System
677 Sciences, 14(10), 1863–1880. https://doi.org/10.5194/hess-14-1863-2010

678 Sprenger, C., Hartog, N., Hernández, M., Vilanova, E., Grützmacher, G., Scheibler, F., &
679 Hannappel, S. (2017). Inventory of managed aquifer recharge sites in Europe: Historical
680 development, current situation and perspectives. Hydrogeology Journal, 25(6), 1909–1922.
681 https://doi.org/10.1007/s10040-017-1554-8

682 Taylor, R.G., Scanlon, B., Döll, P., Rodell, M., Van Beek, R., Wada, Y., Longuevergne, L.,
683 Leblanc, M., Famiglietti, J.S., Edmunds, M. and Konikow, L., 2013. Ground water and climate
684 change. Nature climate change, 3(4), pp.322-329.

685 USGS (United States Geological Survey) 2016 Daily Streamflow Conditions, USGS Current
686 Water Data for the Nation http://waterdata.usgs.gov/nwis/rt

687 Wada, Y., van Beek, L. P., van Kempen, C. M., Reckman, J. W., Vasak, S., & Bierkens, M. F.
688 (2010). Global depletion of groundwater resources. Geophysical Research Letters, 37, L20402.

689 Winter, T.C., J.W. Harvey, O.L. Franke, and W.M. Alley, 1998. Ground Water and Surface
690 Water: A Single Resource. U.S. Geological Survey Circular 1139.
691 http://pubs.water.usgs.gov/cir1139

692 Xiao, M., Koppa, A., Mekonnen, Z., Pagán, B. R., Zhan, S., Cao, Q., Aierken, A., Lee, H. &
693 Lettenmaier, D. P. (2017). How much groundwater did California's Central Valley lose during
694 the 2012–2016 drought?. Geophysical Research Letters, 44(10), 4872-4879.